



OPEN Resveratrol alleviates neuropathic pain associated with restoration of mitochondrial fission–fusion balance in CCI mice

Liu Xie^{1,2,5}, Yiran Xu^{3,5}, Qingqing Yang^{1,2,4}, Wanting Chang^{1,2}, Linna Song^{1,2} & Yanyan Sun^{1,2}✉

Neuropathic pain (NP) is commonly associated with mitochondrial dysfunction in sensory neurons. Although resveratrol (Res), a natural polyphenolic compound, has demonstrated analgesic properties, its impact on mitochondrial dynamics in NP remains unclear. We established a chronic constriction injury (CCI) model in male mice. Starting on the seventh day after the injury, resveratrol (1 mg/kg) or vehicle was administered via intrathecal injection for three consecutive days. We evaluated pain behaviors and analyzed dorsal root ganglia (DRG) for markers of oxidative stress, mitochondrial respiratory chain complexes, fission (DRP1) and fusion (OPA1) proteins, and mitochondrial morphology/ultrastructure. Resveratrol significantly reduced CCI-induced mechanical hypersensitivity and restored thermal latency. In DRG, reactive oxygen species (ROS) accumulation decreased, while superoxide dismutase (SOD) activity increased, indicating reduced oxidative stress. Mitochondrial respiratory chain complexes I–II were restored, while DRP1 expression decreased and OPA1 increased, suggesting a normalization of fission–fusion balance. Resveratrol also increased mitochondrial volume and number. Ultrastructural deficits in mitochondrial area, perimeter, and connectivity were reversed. Resveratrol mitigates CCI-induced NP associated with restoring the balance of mitochondrial fission and fusion proteins and reducing oxidative stress in DRG. These results provide credence to the idea of mitochondrial dynamics as a potential NP target. However, this study did not establish a causal relationship between these molecular changes and resveratrol's analgesic effects through direct manipulation of proteins. Further validation is needed through experiments targeting key proteins involved in mitochondrial fission and fusion.

Keywords DRG, Neuropathic pain, Resveratrol, Mitochondrial, Fission and fusion, Oxidative stress

Neuropathic pain (NP) refers to a persistent pain condition triggered by damage or pathological changes in the somatosensory system, which affects millions of individuals worldwide and significantly reduces quality of life. Common causes include postherpetic neuralgia, diabetic neuropathy, and peripheral nerve injury¹. Current treatments primarily focus on symptom management, but issues such as drug resistance, side effects, and adverse reactions hinder the long-term effectiveness of these therapies. Consequently, novel mechanism-based therapeutic strategies are urgently needed.

Nerve injury triggers the excessive production of reactive oxygen species (ROS), which are crucial in pain signal generation and transmission. ROS contribute through several pathways, including the inflammatory response following peripheral nerve injury, activation of the central nervous system, modulation of signaling pathways, and alteration of ion channel function^{2–4}. Antioxidant therapies targeting ROS have shown potential for pain relief in animal models⁵. Mitochondria serve as the main site for cellular ROS generation⁶. Mitochondrial dysfunction leads to impaired energy metabolism, calcium imbalance, oxidative damage, and dysfunctional mitophagy—all of which promote the progression of NP^{7,8}.

¹Department of Human Anatomy, School of Basic Medicine, Zhengzhou University, Zhengzhou 450001, China.

²Institute of Neuroscience, Zhengzhou University, Zhengzhou 450000, China. ³Henan Key Laboratory of Child Brain Injury and Henan Clinical Research Center for Child Neurological Disorders, Institute of Neuroscience and The Third Affiliated Hospital of Zhengzhou University, Zhengzhou 450015, China. ⁴Patient Case Dept. Storeroom, Xinyang Central Hospital, Xinyang 464000, China. ⁵Liu Xie and Yiran Xu contributed equally to this work. ✉email: yanyansun@zzu.edu.cn

Mitochondrial quality control preserves organelle integrity through biogenesis, selective degradation, and dynamic fission–fusion remodeling⁹. An imbalance between mitochondrial fission and fusion has been identified as a potential underlying cause of NP. Mitochondrial fusion in mammalian cells depends on the activity of mitochondrial fusion proteins 1 and 2 (MFN1 and MFN2), which are specifically localized to the outer mitochondrial membrane (OMM), and optic atrophy 1 (OPA1), which is localized to the inner mitochondrial membrane (IMM). Mitochondrial fission is controlled by three main proteins: dynamin-related protein 1 (DRP1), mitochondrial fission 1 protein (FIS1), and mitochondrial fission factor (MFF)^{10,11}. Studies show that neurons in chronic constriction injury (CCI) models display heightened mitochondrial fragmentation along with reduced mitochondrial density¹². Moreover, pain caused by nerve damage and inflammation resulting from diabetes or chemotherapy significantly enhance mitochondrial fission frequency^{13–15}.

Resveratrol (Res), a natural polyphenol with strong antioxidant and neuroprotective effects, has demonstrated therapeutic potential in several diseases, including Alzheimer's disease¹⁶, epilepsy¹⁷, cardiovascular disease¹⁸, tumors¹⁹, Parkinson's disease²⁰, and neural injury²¹. Res also offers neuroprotection against oxidative stress, inflammation, and mitochondrial dysfunction²². Res exhibits multiple beneficial biological effects; however, at high concentrations, it may induce harmful effects, such as pro-oxidative activity²³. Low-dose administration of RES (1 mg/kg) has been confirmed to have no adverse effects on animal health²⁴. Several studies suggest that Res might help reduce neuropathic pain. In peripheral neuropathic pain, Res inhibits neuroinflammation, activates AMPK, regulates voltage-gated sodium (Nav) 1.7 and potassium channels, and interacts with the serotonergic system²⁵. It can also reduce neuropathic pain from L5/L6 spinal nerve ligation by activating the nitric oxide-cyclic GMP-protein kinase G-large conductance calcium-activated potassium channel pathway²⁶. However, it remains unclear whether Res exerts its antinociceptive effects by restoring mitochondrial fission-fusion balance.

This study investigated the analgesic effects of intrathecal administration of resveratrol on neuropathic pain in CCI mice. Our results demonstrate that Res alleviates neuropathic pain associated with restoring the balance of mitochondrial fission and fusion in DRG of CCI mice. Additionally, Res reduces oxidative stress, mitigates mitochondrial dysfunction, and provides new insights into the preclinical mechanisms of resveratrol in CCI-induced NP.

Materials and methods

Animals

Adult male C57BL/6 mice (20–25 g) were obtained from Beijing SPF Biotechnology Co., Ltd. and handled following the Zhengzhou University Guidelines for the Care and Use of Laboratory Animals. Mice were kept in regulated environments: temperature ranged from 20 to 26 °C, humidity was maintained at 40–70%, and a 12-hour cycle of light and darkness was maintained. The air was purified and filtered, and the facility was regularly ventilated. Cages were clean, non-toxic, and maintained at appropriate densities. Bedding was replaced daily, and both drinking water and food were sterile and nutritionally balanced. All animal procedures received approval from the Animal Ethics Committee of Zhengzhou University (Ethics Number: ZZUIRB2022-48), and the study adhered strictly to laboratory animal ethics guidelines. The experimental methods followed the ARRIVE guidelines and other relevant regulations.

Surgical procedures of the CCI model

The chronic constriction injury (CCI) model of the sciatic nerve was established to induce sciatic NP in mice, following a previously described protocol with minor modifications²⁷. Mice were anesthetized with isoflurane (5% for induction and 1.5–3.0% for maintenance), positioned in a lateral decubitus posture, and the surgical area was disinfected with an alcohol wipe. A 1.5 cm cut was made on the left thigh, and the biceps femoris muscle was carefully separated along its fibers to expose the primary trunk of the sciatic nerve. Using hemostatic forceps, we carefully isolated the nerve. The sciatic nerve was subsequently ligated at three locations, spaced 0.5–1 mm apart, using a 6–0 suture thread. The ligature was tightened to the point where slight twitching of the calf muscle or toes was observed when the knot was tied. After ligation, the muscle and skin were sutured, and the incision was first sterilized with povidone-iodine, followed by 70% ethanol. Age-matched control mice from the same litter were randomly selected and underwent no nerve ligation procedure.

Von Frey test

We assessed mechanical pain sensitivity by observing the paw withdrawal reaction to von Frey filament stimulation. Mice were positioned on a metal mesh rack, separated by a test cage. The animals were allowed to acclimate for 30–60 min until they are calm and motionless. The hind paws were first stimulated with a 0.07 g von Frey filament, with 10 stimulations per paw and at least a 5-minute interval between stimulations. After the 0.07 g stimulation, we used a 0.4 g von Frey filament for further testing. A positive response, such as a brisk withdrawal, licking, or flutter, was recorded. The paw withdrawal frequency (PWF) was calculated as: % = (positives/10) × 100.

Hargreaves test

We measured the latency of paw withdrawal in response to radiant heat using an infrared thermal pain tester (Ugo Basile, Varese, Italy). Mice were placed in an organic plastic container on a glass surface, with the room temperature maintained at 23–25 °C. They were allowed to acclimate for 30–60 min until they were calm and ready for testing. The heat source was placed beneath the bottom surface of the hind paw, and infrared light was used to deliver the stimulus. We set the baseline latency for normal mice at 10–12 s, which corresponds to the intensity of the infrared beam. The radiation cutoff time was established at 20 s to prevent potential tissue damage if the mouse did not respond. We recorded three measurements for each paw, with at least a ten-minute

interval between each test. During each test, we observed the mouse's injury response, such as paw licking or jumping. Finally, we calculated the average withdrawal latency for each hind paw based on the recorded values.

Western-blot

We lysed mouse L3-L5 DRG tissue using a cytoplasmic lysis buffer supplemented with protease inhibitors. Collected the supernatant and measured the protein concentration using the BCA protein quantification kit (SolaBio, China). Sample was separated by 10% sodium dodecyl sulfate-polyacrylamide gel electrophoresis (SDS-PAGE), followed by electrotransfer onto a polyvinylidene difluoride (PVDF) membrane. To block nonspecific binding, the membrane was incubated with 5% bovine serum albumin (BSA) for 2 h at room temperature. It was then incubated overnight at 4 °C with the primary antibody. The antibodies listed below were utilized: mouse anti-OPA1 (1:1000, BD Biosciences, 612606), rabbit anti-DRP1 (1:1000, Abcam, AB184247), rabbit anti- β -actin (1:1000, Servicebio, GB11001), mouse anti-GAPDH (1:2000, Servicebio, GB11002), rabbit anti-CI-NDUFB8 (1:5000, Proteintech, 14794-1-AP), rabbit anti-CII-SDHB (1:8000, Proteintech, 10620-1-AP), rabbit anti-CIII-UQCRC2 (1:4000, Proteintech, 14742-1-AP), rabbit anti-CIV-MTCO2 (1:1000, Proteintech, 55070-1-AP), and rabbit anti-CV-ATP5A1 (1:8000, Proteintech, 14676-1-AP). Next, the membrane was incubated with a rabbit or mouse secondary antibody (1:10,000 dilution; Abbkine, China) at room temperature for 2 h. After washing with TBST, the membrane was visualized using a gel imaging and analysis system. During the analysis, we used ImageJ software to measure the gray values for each channel. GAPDH or β -actin served as the loading controls for normalization. To calculate the relative protein expression, we calculated the ratio of the target protein's grayscale value to that of the reference protein. We then averaged control group data and standardized the results by dividing each group's value by the control average.

Electron microscopy

L3-L5 DRG tissue was collected from mice following perfusion with 4% paraformaldehyde (PFA) and 4% glutaraldehyde. The tissue was then fixed in 2.5% glutaraldehyde. Following fixation, samples were rinsed with 0.1 M phosphate-buffered saline (PBS) and stained with 1% osmium tetroxide (TED PELLA, catalog number 18451) for 1.5 h. Subsequently, a gradient of ethanol concentrations (50%, 70%, 90%, 100%) was used in a sequential manner to dehydrate the samples, after which propylene oxide was applied. The tissue was subsequently embedded in epoxy resin and left to cure overnight at room temperature. Ultrathin slices measuring 70 nm were prepared using an ultramicrotome. Double staining of the sections was performed using 3% uranyl acetate and lead citrate, followed by examination with a transmission electron microscope. Image acquisition was performed by a technician blinded to the experimental conditions. Mitochondrial morphology, including perimeter and area, was analyzed using Image-Pro Plus software.

Immunofluorescence

For immunofluorescence staining, mice were first perfused with physiological saline, followed by injection of 4% polyformaldehyde (PFA). The L3-L5 segment DRG tissue was removed and fixed in 4% PFA overnight at 4 °C. After fixation, the tissue was dehydrated with sucrose and embedded in OCT, sectioned into 12 μ m slices, and mounted on glass slides. Incubated frozen sections in PBS containing 10% goat serum and 0.3% Triton X-100 at 37 °C for 2 h. Primary antibodies were then applied: mouse anti-OPA1 (1:200, BD Biosciences, 612606) and rabbit anti-DRP1 (1:200, Abcam, AB184247) and incubated at 37 °C for 2–3 h. Afterward, the sections were incubated for 2 h at room temperature in the dark with secondary antibodies: Cy3-labeled goat anti-rabbit (1:200, Jackson ImmunoResearch) and 488-labeled goat anti-mouse (1:200, Jackson ImmunoResearch). Fluorescent signals were detected using an upright fluorescence microscope (Olympus Corporation, Japan). Image analysis was performed using ImageJ software. Optimized threshold settings fully enclosed the target signals while excluding background interference, allowing for accurate statistical calculation of average fluorescence intensity.

Intrathecal injection

Mice were anesthetized with isoflurane, and once under deep anesthesia, the lumbar spine was positioned in a kyphotic posture to increase the inter-spinous space. Using a Hamilton micro syringe (10 μ l needle, 0.26 mm gauge), we aspirated either resveratrol (1 mg/kg) or Mitotracker™ Deep Red probe (10 μ l, 100 nM) and injected it into the L5-L6 intervertebral space. Resveratrol was dissolved in 100% dimethyl sulfoxide (DMSO) at a final concentration of 2.5 mg/ml. Successful insertion was confirmed when the mouse exhibited a distinct tail-flicking response. DRG frozen sections were cut at a thickness of 12 μ m, with Z-stacks covering a depth of 10 μ m. The inter-slice spacing was 1 μ m per layer, resulting in 10 consecutive Z-slices. The pixel resolution was 512 \times 512 pixels. Quantitative analysis was performed using the ImageJ “3D Objects Counter” plugin. Threshold settings were optimized to fully capture the target mitochondrial signals while excluding background noise, allowing for statistical quantification of mitochondrial volume and number.

DHE staining

To assess ROS levels in DRG tissue, we used a dihydroethidine (DHE) fluorescent probe. Frozen DRG sections were incubated with DHE solution (1.25 μ g/ml) at 37 °C for 30 min. Fluorescent signals were detected using a fluorescence microscope (Olympus Corporation, Japan), and image analysis was performed using ImageJ software.

SOD activity detection

SOD activity in DRG tissue was measured using the Total SOD Colorimetric Assay Kit (Elabscience, catalog No. E-BC-K020-M). The assay was conducted according to the manufacturer's instructions, and the optical density (OD) was recorded at 450 nm. SOD activity was calculated when the inhibition rate was between 25% and 65%.

Statistical analysis

We analyzed the data using GraphPad Prism (v8.3.0). Results are presented as mean \pm standard deviation (SD). To compare two independent groups, we applied an unpaired two-tailed t-test, or the Mann–Whitney test if the data were not normally distributed. For univariate analyses with more than two groups, we applied a one-way ANOVA when the data were normally distributed with equal variances, followed by Tukey's test for multiple comparisons. If the data were not normally distributed, we applied the Kruskal–Wallis test. For multivariate comparisons, we employed a two-way ANOVA when the data met the assumptions of normality and equal variances, followed by Sidak's test for multiple comparisons. $p < 0.05$ represents statistically significant.

Results

Res alleviates pain symptoms in CCI mice

We first established a CCI model to investigate the effects of Res on neuropathic pain (Fig. 1A). Res was administered intrathecally at a dose of 1 mg/kg once daily for three consecutive days, beginning on the seventh day post-CCI. To assess mechanical sensitivity (paw withdrawal frequency, PWF) and thermal sensitivity (thermal withdrawal latency), we conducted the Von Frey test and thermal pain measurements (Fig. 1B). Behavioral data are shown in Table 1. These results show that, compared to the Sham + DMSO group, the CCI group exhibited a significant increase in mechanical withdrawal frequency and a decrease in thermal withdrawal latency on day 7 post-CCI, which indicates the emergence of mechanical and thermal pain hypersensitivity. Intrathecal injection of resveratrol significantly alleviated CCI-induced mechanical and thermal pain hypersensitivity (Fig. 1C–E). However, no notable changes were observed in the contralateral mechanical foot withdrawal frequency or

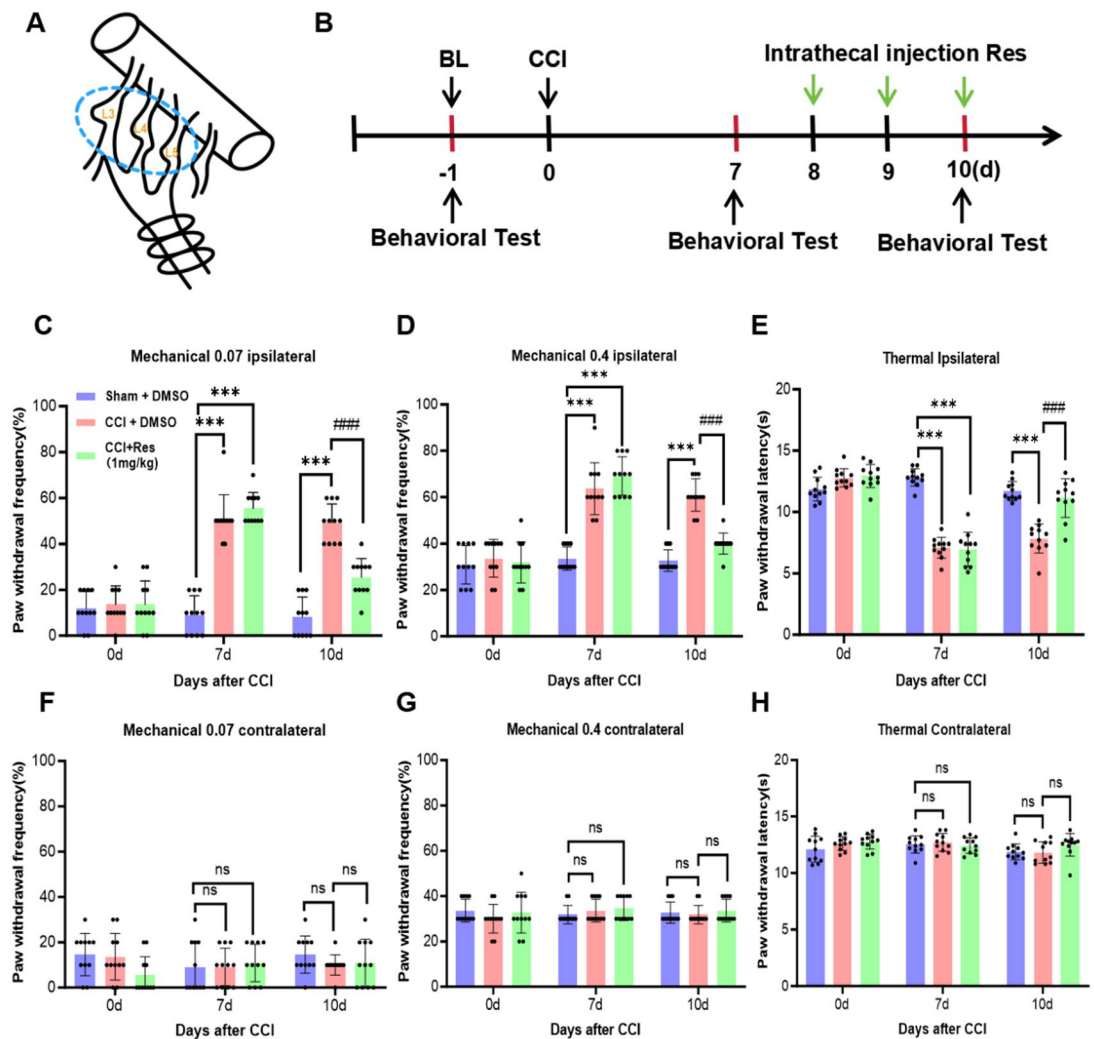


Fig. 1. Intrathecal injection of resveratrol alleviates pain symptoms in CCI mice. (A) Schematic of the CCI model. (B) Experimental workflow of the intrathecal injection of resveratrol. (C,D) Mechanical paw withdrawal frequency on the operated side of mice at 0.07 g and 0.4 g. (E) Latency of thermal foot withdrawal on the operated side of the mice. (F,G) Mechanical paw withdrawal frequency on the contralateral side of mice at 0.07 g and 0.4 g. (H) Latency to thermal foot withdrawal on the contralateral side of the mice. Two-way ANOVA, *** $p < 0.001$ vs. Sham + DMSO, ### $p < 0.001$ vs. CCI + DMSO, $n = 11$ per group.

	Sham + DMSO			CCI + DMSO			CCI + Res		
	0d	7d	10d	0d	7d	10d	0d	7d	10d
0.07 g mechanical foot withdrawal frequency	11.667 ± 7.177%	8.333 ± 8.348%	7.500 ± 8.660%	14.167 ± 7.930%	50.000 ± 10.445%	49.167 ± 7.930%	13.636 ± 10.269%	55.455 ± 6.876%	25.455 ± 8.202%
0.4 g mechanical foot withdrawal frequency	30.833 ± 7.930%	33.33 ± 4.924%	32.50 ± 4.523%	33.333 ± 7.785%	63.333 ± 10.731%	60.833 ± 6.868%	31.818 ± 8.739%	69.091 ± 8.312%	40.000 ± 4.472%
thermal foot withdrawal latency	11.900 ± 0.943s	12.65 ± 0.89s	11.69 ± 0.74s	12.900 ± 0.837s	7.142 ± 0.817s	7.950 ± 1.196s	12.927 ± 0.943s	6.964 ± 1.37s	11.127 ± 1.58s

Table 1. Behavioral data.

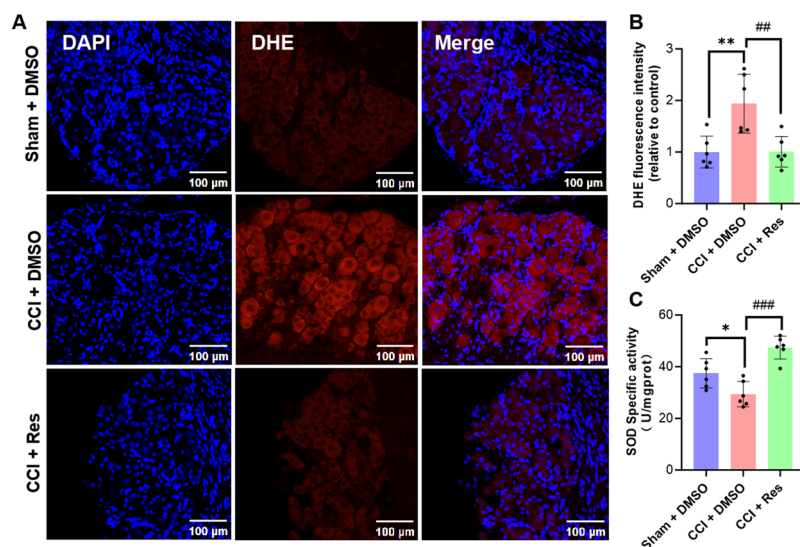


Fig. 2. Intrathecal injection of resveratrol alleviates oxidative stress damage in CCI mice. **(A)** DHE assay showing ROS levels in the DRG of each group. **(B)** Average fluorescence intensity of DHE-positive cells in the DRG. One-way ANOVA, $**p < 0.01$ vs. Sham + DMSO, $##p < 0.01$ vs. CCI + DMSO, $n = 6$ per group, Scale bars = 100 μ m. **(C)** SOD activity. One-way ANOVA, $*p < 0.05$ vs. Sham + DMSO, $###p < 0.001$ vs. CCI, $n = 6$ /group.

thermal foot withdrawal latency (Fig. 1F–H), suggesting that resveratrol specifically reduces tactile allodynia associated with neuropathic pain in the CCI model.

Res alleviates oxidative stress damage in CCI mice

Previous studies have demonstrated that ROS levels increase in neurons following.

pain-induced injury²⁸. In this study, we used the fluorescent probe DHE to assess ROS levels in tissue. The staining results revealed that ROS levels were significantly elevated in the DRG of CCI mice compared to the sham + DMSO group. Intrathecal injection of resveratrol significantly reduced CCI-induced ROS accumulation (CCI + DMSO: 1.940 ± 0.571 , CCI + Resveratrol: 1.006 ± 0.298 , $p < 0.01$) (Fig. 2A–B). Cellular redox status is regulated by the balancing oxidative and antioxidant systems and involving various enzymes. SOD, an essential antioxidant enzyme, plays a vital role in protecting cells against oxidative stress²⁹. SOD activity was measured in DRG from each group. The results showed a decrease in SOD activity following CCI, while resveratrol treatment increased SOD activity (Sham + DMSO: 37.45 ± 5.654 , CCI + DMSO: 29.41 ± 4.919 , CCI + Resveratrol: 47.43 ± 4.429 , $p < 0.001$) (Fig. 2C). These findings suggest that resveratrol mitigates CCI-induced oxidative stress.

Res increases the expression of mitochondrial complexes I and II in CCI mice

The primary source of ROS is the mitochondrial respiratory chain, where ROS generation is associated with electron leakage. Complexes I–V are essential components of this chain. This study assessed the expression of these mitochondrial complexes in the DRG following CCI. Western blot analysis showed that the levels of mitochondrial complexes I and II were significantly lower in the CCI + DMSO group compared to the

Sham + DMSO group. However, treatment with resveratrol upregulated the expression of these complexes (mitochondrial complexes I, CCI + DMSO: 0.526 ± 0.187 , CCI + Resveratrol: 0.877 ± 0.139 , $p < 0.05$; mitochondrial complexes II, CCI + DMSO: 0.676 ± 0.276 , CCI + Resveratrol: 1.008 ± 0.258 , $p < 0.05$) (Fig. 3A–B). There were no notable differences in the expression levels of mitochondrial complexes III (CCI + DMSO: 1.013 ± 0.204 , CCI + Resveratrol: 1.146 ± 0.230), IV (CCI + DMSO: 1.069 ± 0.622 , CCI + Resveratrol: 0.813 ± 0.394), or V (CCI + DMSO: 1.004 ± 0.196 , CCI + Resveratrol: 1.049 ± 0.209) between the experimental groups (Fig. 3C–E). These findings suggest that resveratrol selectively restores the expression of damaged mitochondrial complexes I and II in the CCI model, thus improving mitochondrial function.

Resveratrol reduces expression of the mitochondrial fission protein DRP1 in the DRG of CCI mice and increases expression of the fusion protein OPA1

Mitochondrial function and morphology are maintained by the processes of mitochondrial fission and fusion. DRP1 promotes mitochondrial fission, while OPA1 is involved in inner membrane fusion. Compared to the Sham + DMSO group, CCI mice exhibited elevated DRP1 levels and reduced OPA1 levels in the ipsilateral DRG. Resveratrol treatment significantly suppressed the CCI-induced increase in DRP1 (CCI + DMSO:

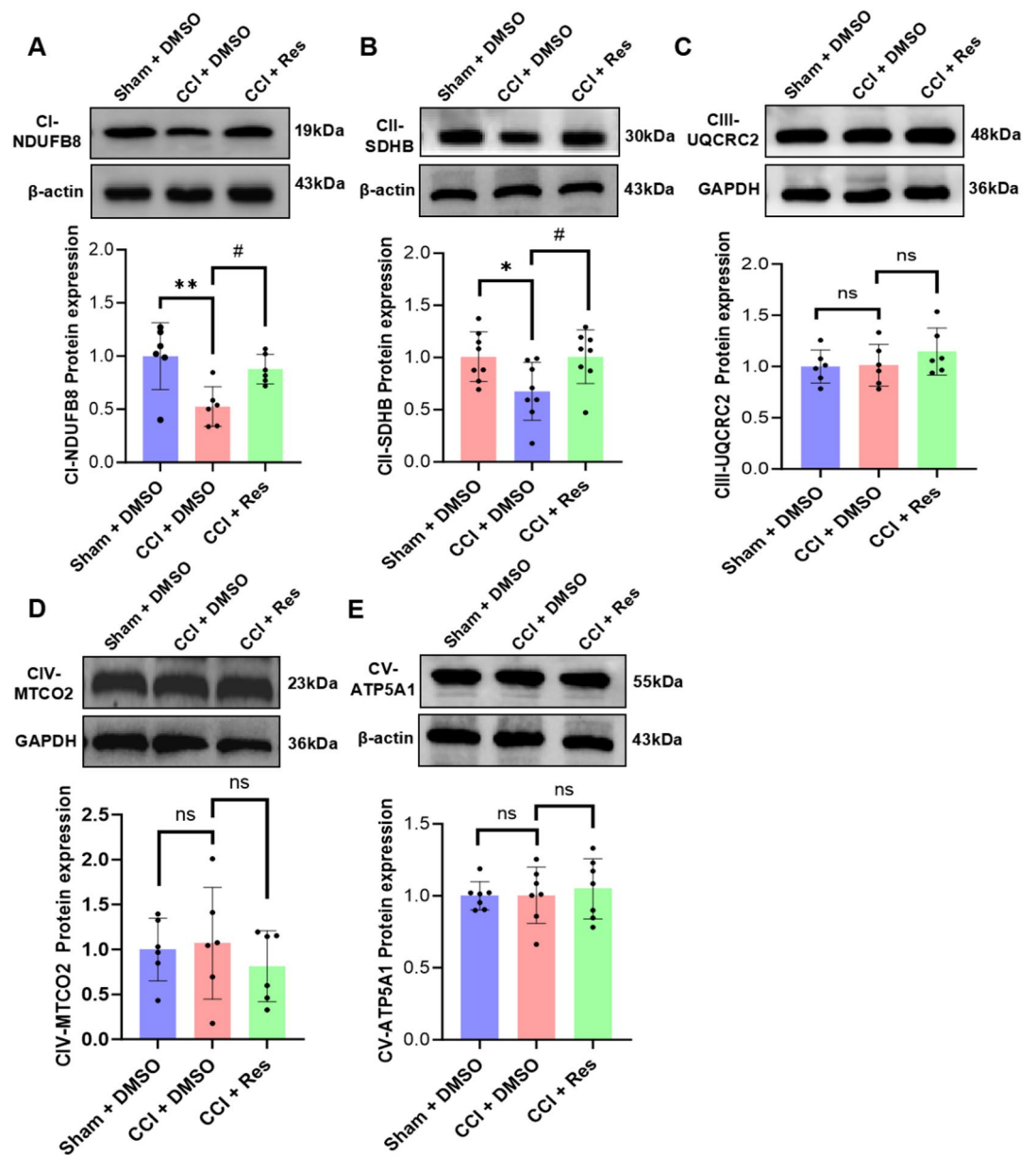


Fig. 3. Res increases the expression of mitochondrial complexes I and II in CCI mice. (A–E) Changes to CI-DNUFB8 ($n = 6$ per group), CII-SDHB ($n = 8$ per group), CIII-UQCRC2 ($n = 6$ per group), CIV-MTCO2 ($n = 6$ per group), CV-ATP5A1 ($n = 7$ per group) protein expression in each group. One-way ANOVA, $*p < 0.05$, $**p < 0.01$ vs. Sham + DMSO, $\#p < 0.05$ vs. CCI + DMSO.

1.580 ± 0.595, CCI + Resveratrol: 0.887 ± 0.183, $p < 0.05$) and the decrease in OPA1 (CCI + DMSO: 0.464 ± 0.195, CCI + Resveratrol: 0.886 ± 0.375, $p < 0.05$) (Fig. 4A). Immunofluorescence analysis confirmed that, compared to Sham + DMSO, DRP1 fluorescence intensity was higher, and OPA1 intensity was lower in CCI mice. Resveratrol treatment reversed these changes (Fig. 4B-C). OPA1 localizes to the inner mitochondrial membrane, with its fluorescence distribution regulated by mitochondrial targeting. In DRG large ganglion neurons, mitochondria are enriched in the perinuclear region and axon initiation zone, while being sparse in the central soma. Consequently, OPA1 signal exhibits a hollow ring-like pattern with strong peripheral and weak central intensity. DRP1, a cytoplasmic GTPase, freely shuttles between the cytoplasm and mitochondrial outer membrane. Its distribution is independent of mitochondrial localization, resulting in a uniform cytoplasmic signal. These findings suggest that resveratrol can restore mitochondrial dynamic balance by correcting CCI-induced fission-fusion imbalances.

Resveratrol improves mitochondrial morphological abnormalities in DRG induced by CCI

Mitochondrial fission and fusion significantly influence the number, size, and morphology of mitochondria. Altered expression of fission and fusion proteins may contribute to changes in mitochondrial characteristics following CCI. To examine this, we used the mitochondrial fluorescent probe Mitotracker™ Deep Red to label mitochondria in DRG and assess their subcellular morphology. In the sham + DMSO group, mitochondria formed a well-organized, interconnected network. However, in the CCI + DMSO group, mitochondria were fragmented and appeared as small, dispersed granules (Fig. 5A). Quantitative analysis revealed that the mitochondrial volume in DRG in the CCI + DMSO group decreased, while the mitochondrial number increased. After resveratrol treatment, mitochondrial volume in DRG significantly increased (CCI + DMSO: 0.651 ± 0.126, CCI + Resveratrol: 0.971 ± 0.188, $p < 0.001$) (Fig. 5B), and the number of mitochondria returned to levels similar to those in the Sham + DMSO group (Sham + DMSO: 16.17 ± 7.420, CCI + DMSO: 25.13 ± 9.285, CCI + Resveratrol: 17.52 ± 7.480, $p < 0.001$) (Fig. 5C). These results suggest that resveratrol can improve mitochondrial morphological abnormalities in DRG induced by CCI.

To further assess mitochondrial morphology following CCI, we employed transmission electron microscopy to examine the mitochondrial ultrastructure (Fig. 6A). We focused on three key parameters: mitochondrial circumference (μm), mitochondrial area (μm²), and interconnectivity score (calculated as mitochondrial area/circumference, with a lower ratio indicating fragmentation). The results revealed that, compared to the Sham + DMSO group, CCI led to a reduction in mitochondrial area, a shortened perimeter, and decreased connectivity in DRG, indicating excessive mitochondrial fragmentation. After resveratrol treatment, mitochondrial area in DRG increased (Sham + DMSO: 0.145 ± 0.092 μm², CCI + DMSO: 0.061 ± 0.047 μm², CCI + Resveratrol: 0.139 ± 0.103 μm², $p < 0.001$) (Fig. 6B). The mitochondrial perimeter also increased (Sham + DMSO: 1.532 ± 0.651 μm, CCI + DMSO: 0.910 ± 0.388 μm, CCI + Resveratrol: 1.471 ± 0.675 μm, $p < 0.001$) (Fig. 6C), as did mitochondrial interconnectivity (Sham + DMSO: 0.089 ± 0.022, CCI + DMSO: 0.060 ± 0.018, CCI + Resveratrol: 0.086 ± 0.023, $p < 0.001$) (Fig. 6D). These findings suggest that resveratrol can ameliorate CCI-induced mitochondrial morphological abnormalities in DRG by restoring mitochondrial dynamic balance, inhibiting excessive fission, and promoting fusion, ultimately improving mitochondrial structure and function.

Discussion

This study investigated the neuroprotective effects of intrathecal resveratrol on DRG following CCI. We first observed that CCI-induced pain behavior was linked to significant disruptions in mitochondrial dynamics within the DRG. These disruptions included increased expression of the mitochondrial fission protein DRP1, decreased levels of the fusion protein OPA1, and elevated ROS production. Ultrastructural analysis revealed a decrease in mitochondrial area, perimeter, and network connectivity, accompanied by a shift toward fragmented, rounded morphologies. Next, we found that intrathecal resveratrol injection alleviated CCI-induced pain behavior. Mitochondrial labeling with Mitotracker Deep Red showed that resveratrol treatment mitigated the reduction in mitochondrial volume and the increase in mitochondrial number in DRG following CCI. Ultrastructural analysis further demonstrated that resveratrol significantly restored mitochondrial area, perimeter, and interconnectivity in DRG of CCI mice. Additionally, resveratrol alleviated CCI-induced oxidative stress and restored mitochondrial function. Although this study did not directly validate causality by modulating DRP1 or OPA1, our previously published research¹² confirmed that targeted regulation of DRP1 or OPA1 effectively modulates neuropathic pain, indicating that resveratrol may alleviate neuropathic pain by improving mitochondrial function, potentially via the regulation of mitochondrial fission and fusion balance in the CCI model.

Resveratrol has been identified as a potential treatment option for various health conditions, including cancer³⁰, pain³¹, inflammation³², tissue damage³³, and other diseases³⁴. Resveratrol has shown promise in alleviating abnormal neuropathic pain in animal models of L5/L6 spinal nerve ligation and diabetic neuropathy^{35,36}. In rats with chronic sciatic nerve compression injury, resveratrol reduced pain in a dose-dependent way by inhibiting pro-inflammatory cytokines (IL-1β, IL-6, TNF-α) and enhancing the production of the anti-inflammatory cytokine IL-10. The analgesic effects were most pronounced when administered 7 days post-injury³⁷. In our study, we further confirmed resveratrol's potential in treating neuropathic pain, demonstrating that intrathecal resveratrol administration significantly alleviated CCI-induced neuropathic pain in mice.

ROS are highly reactive free radicals, primarily superoxide anions, produced when molecular oxygen accepts an electron. Oxidative stress is especially problematic for neurons due to their high oxygen demand. Excessive ROS can impair presynaptic inhibitory input to the spinal cord, inhibit the release of gamma-aminobutyric acid (GABA), and activate NMDA and AMPA receptors, leading to central sensitization and the progression of neuropathic pain³⁸. Earlier research has shown that resveratrol, a potent antioxidant and free radical scavenger, mitigates several pathological features associated with neuropathic pain^{39,40}. In a rat model of mechanical pain

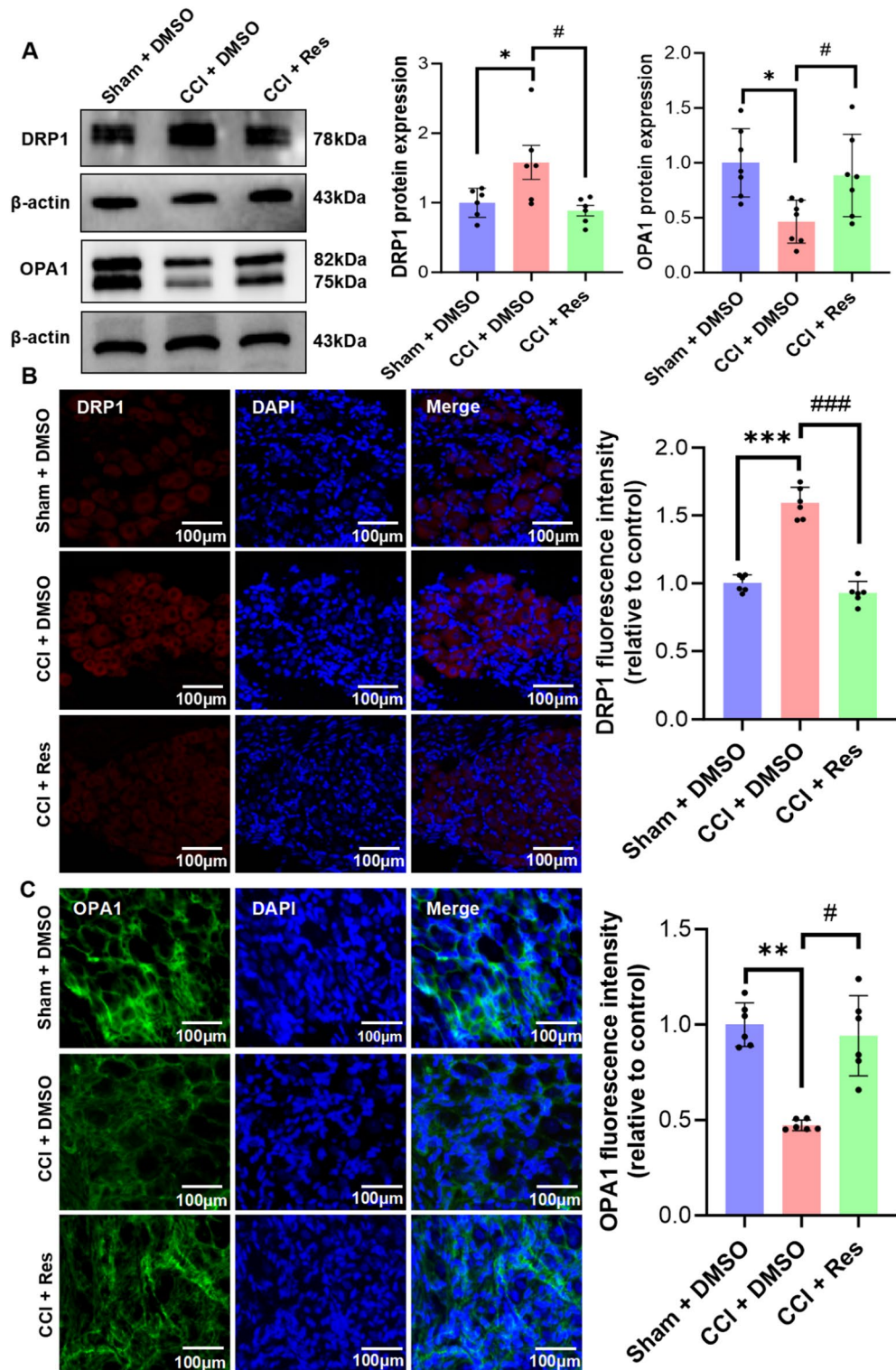


Fig. 4. Resveratrol reduces expression of the mitochondrial division protein DRP1 and increases expression of the fusion protein OPA1 in the DRG of CCI mice. (A) Changes to DRP1 and OPA1 protein levels. (B) Average fluorescence intensity of DRP1. (C) Average fluorescence intensity of OPA1. One-way ANOVA, * $p < 0.05$, ** $p < 0.01$, *** $p < 0.001$ vs. Sham + DMSO, # $p < 0.05$, ### $p < 0.001$ vs. CCI + DMSO, $n = 6$ per group. Scale bars, 100 μm .

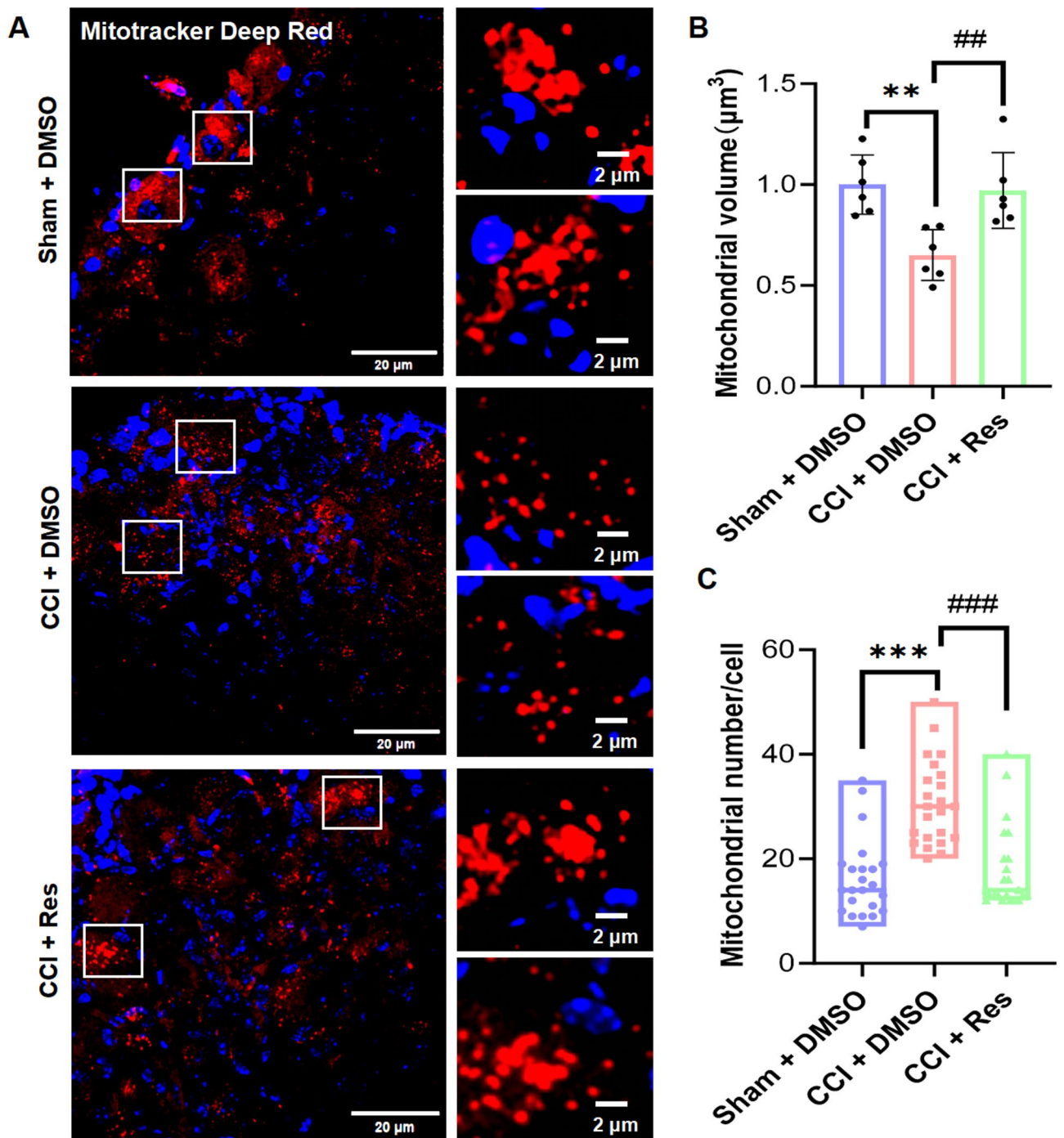


Fig. 5. Resveratrol improves mitochondrial morphological abnormalities in CCI-induced DRG (A) Mitotracker Deep Red-stained representative confocal microscopy images of mitochondrial morphology. Scale bars, 20 μ m. (B) Average mitochondrial volume in DRG across groups. One-way ANOVA, ** $p < 0.01$ vs. Sham + DMSO, ** $p < 0.01$ vs. CCI + DMSO, $n = 6$ per group. (C) Number of mitochondria per cell in DRG across groups. Kruskal-Wallis test, *** $p < 0.001$ vs. Sham + DMSO, *** $p < 0.001$ vs. CCI + DMSO, $n = 23$ cells.

induced by complete Freund's adjuvant, blocking the cyclooxygenase-2 (COX-2) pathway was found to reduce prostaglandin E2 production and suppress the overactivity of neurons in the caudal nucleus of the trigeminal spinal tract, thereby alleviating trigeminal neuralgia⁴¹. In the current study, we confirmed resveratrol's antioxidant properties. Specifically, intrathecal administration of resveratrol significantly reduced ROS accumulation induced by CCI and enhanced SOD activity, thereby alleviating CCI-induced neuropathic pain.

Mitochondria are the primary source of ROS⁴². Neurons, with their complex morphology and high energy demands, are especially vulnerable to mitochondrial dysfunction^{43,44}. Res has been shown to reduce the expression of vascular endothelial growth factor (VEGF) and hypoxia-inducible factor 1-alpha (HIF-1 α), induce T-cell

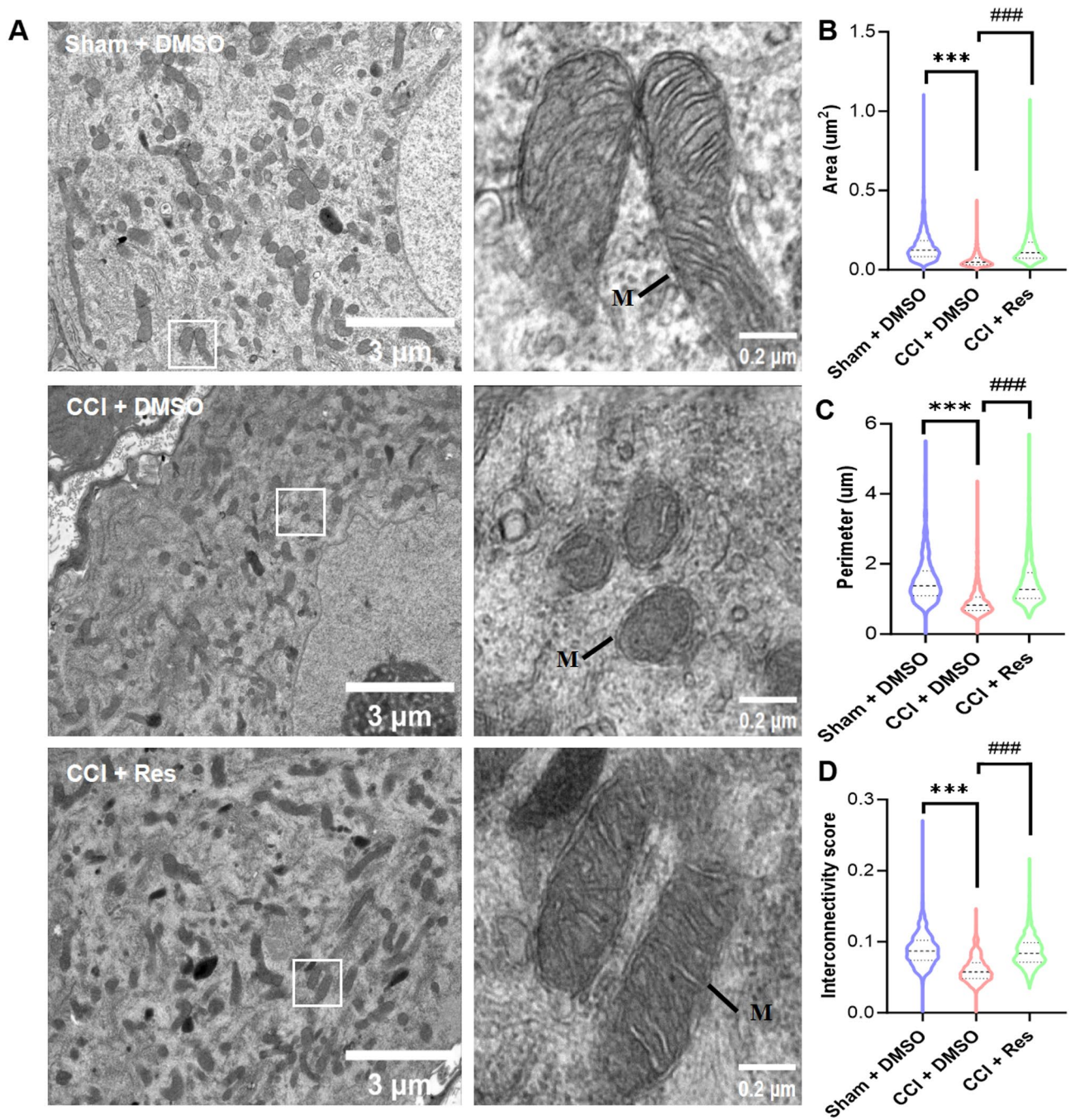


Fig. 6. Resveratrol improves mitochondrial morphological abnormalities in CCI-induced DRG. **(A)** Electron micrographs of mitochondria in DRG from each group. Scale bars, 3 μm. **(B)** Mitochondrial areas in DRG from each group. **(C)** Mitochondrial perimeters in DRG from each group. **(D)** Mitochondrial interconnectivity of DRG from each group. Kruskal-Wallis test, *** $p < 0.001$ vs. Sham + DMSO, ### $p < 0.001$ vs. CCI + DMSO, M represents mitochondria, $n = 1,035$ mitochondria.

apoptosis, suppress the production of interleukin-17 (IL-17) and other inflammatory molecules, and activate key regulators of mitochondrial function⁴⁵, including SIRT1 and PGC-1 α . Mitochondrial complexes I–V are essential components of the mitochondrial respiratory chain⁴⁶, which is crucial for cellular energy production. In this study, we observed that CCI reduced the expression of mitochondrial complexes I and II, whereas resveratrol treatment restored their levels. These findings suggest that resveratrol can correct mitochondrial respiratory chain abnormalities, potentially improving electron transport and ATP synthesis efficiency. The processes of mitochondrial fission and fusion are essential for maintaining mitochondrial function. Disruptions in this balance, such as excessive fragmentation, swelling, vacuolation, reduced cristae, or a fragmented network, have been linked to various neurological disorders[47–49]. In the paclitaxel-induced NP model, swelling and vacuole

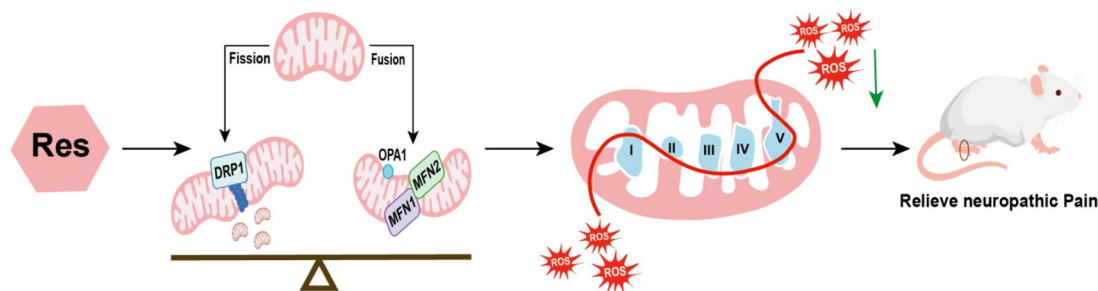


Fig. 7. Schematic of resveratrol regulation of neuropathic pain. Res alleviates neuropathic pain associated with maintaining a balance of mitochondrial fission and fusion in CCI mice, reducing oxidative stress damage. MFN1 and MFN2 are key components of the mitochondrial fusion machinery and included in the schematic for mechanistic completeness, while their expression was not measured in the present study.

formation were observed in the mitochondria within the axons of the oculomotor nerve. The incidence of these abnormalities increased significantly in the axons of both A fibers and C fibers[50]. Similarly, in the sciatic nerve branch selective injury (SNI) model, mitochondrial number increased, but the mitochondrial circumference and area decreased, with a shift toward more circular shapes and enlarged vacuoles[51]. In this study, we evaluated both mitochondrial protein expression and ultrastructural morphology. Our results confirm that intrathecal resveratrol treatment reduced mitochondrial fragmentation and promoted mitochondrial fusion in DRG of CCI mice, reestablishing the equilibrium between fission and fusion(Fig. 7). These results emphasize the important role of mitochondrial dynamics in the progression of neuropathic pain and suggest that resveratrol may act as a regulator of mitochondrial homeostasis.

However, certain limitations must be acknowledged. (1) This study used only one animal model and dosing schedule, which limits its ability to fully represent the analgesic effects of resveratrol across various causes and sexes, as well as the complexity of clinical neuropathic pain. (2) Additionally, by evaluating only short-term effects at 10 days after surgery, it did not examine long-term outcomes or possible off-target effects, thus lacking adequate evidence for the safety and effectiveness of extended clinical use. (3) The absence of direct mitochondrial function assays hinders the verification of resveratrol's beneficial effects on mitochondrial function in DRG. (4) Since DRG tissue contains multiple cell types, it remains unclear whether the observed mitochondrial and protein changes are neuron-specific.

In this study, we identified mitochondrial dynamics as a potential therapeutic target for treating neuropathic pain. Our findings suggest that resveratrol, or similar compounds, may offer a translational approach for treatment based on its mechanisms of action.

Data availability

The data underlying the findings of this study are available from the corresponding author upon reasonable request.

Received: 4 October 2025; Accepted: 24 February 2026

Published online: 04 March 2026

References

1. Finnerup, N. B., Kuner, R. & Jensen, T. S. Neuropathic pain: From mechanisms to treatment. *Physiol. Rev.* **101**(1), 259–301 (2021).
2. Cheng, X. et al. Mitochondria-targeting bimetallic cluster nanozymes alleviate neuropathic pain through scavenging ROS and reducing inflammation. *Adv. Healthc. Mater.* **14**(8), e2401607 (2025).
3. Mandlem, V. K. K. et al. TLR4 induced TRPM2 mediated neuropathic pain. *Front. Pharmacol.* **15**, 1472771 (2024).
4. Zhang, W. et al. Spinal AT1R contributes to neuroinflammation and neuropathic pain via NOX2-dependent redox signaling in microglia. *Free Radic Biol. Med.* **227**, 143–156 (2025).
5. Xu, Z. et al. The role of antioxidant therapy in modulating neuropathic pain: A systematic review of mechanistic insights and research trends (2003–2024). *Brain Circ.* **11**(2), 113–126 (2025).
6. Palma, F. R. et al. ROS production by mitochondria: Function or dysfunction?. *Oncogene* **43**(5), 295–303 (2024).
7. Chan, D. C. Mitochondrial dynamics and its involvement in disease. *Annu. Rev. Pathol.* **15**, 235–259 (2020).
8. Vazquez-Trincado, C. et al. Mitochondrial dynamics, mitophagy and cardiovascular disease. *J. Physiol.* **594**(3), 509–25 (2016).
9. Palmeira, C. M. et al. Mitohormesis and metabolic health: The interplay between ROS, cAMP and sirtuins. *Free Radic. Biol. Med.* **141**, 483–491 (2019).
10. Ma, Y., Wang, L. & Jia, R. The role of mitochondrial dynamics in human cancers. *Am. J. Cancer Res.* **10** (5), 1278–1293 (2020).
11. Pernas, L. & Scorrano, L. Mitochondrial fusion, fission, and cristae remodeling as key mediators of cellular function. *Annu. Rev. Physiol.* **78**, 505–531 (2016).
12. Xie, L. et al. Mechanistic study of modulating mitochondrial fission and fusion to ameliorate neuropathic pain in mice. *Sci. Rep.* **15**(1), 15571 (2025).
13. George, D. S. et al. Mitochondrial calcium uniporter deletion prevents painful diabetic neuropathy by restoring mitochondrial morphology and dynamics. *Pain* **163** (3), 560–578 (2022).
14. Doyle, T. M. & Salvemini, D. Mini-review: Mitochondrial dysfunction and chemotherapy-induced neuropathic pain. *Neurosci. Lett.* **760**, 136087 (2021).
15. Xie, M. et al. 2-bromopalmitate attenuates inflammatory pain by maintaining mitochondrial fission/fusion balance and function. *Acta Biochim. Biophys. Sin. (Shanghai)* **53**(1), 72–84 (2021).

16. Subhan, I. & Siddique, Y. H. Resveratrol: Protective agent against Alzheimer's disease. *Cent Nerv Syst Agents Med Chem* **24**(3), 249–263 (2024).
17. Lu, S. & Wang, X. The role and potential mechanism of resveratrol in the prevention and control of epilepsy. *Future Med. Chem.* **7**(15), 2005–2018 (2015).
18. Raj, P., Zieroth, S. & Netticadan, T. An overview of the efficacy of resveratrol in the management of ischemic heart disease. *Ann. N. Y. Acad. Sci.* **1348**(1), 55–67 (2015).
19. Mu, Q. & Najafi, M. Resveratrol for targeting the tumor microenvironment and its interactions with cancer cells. *Int. Immunopharmacol.* **98**, 107895 (2021).
20. Kung, H. C. et al. Oxidative stress, mitochondrial dysfunction, and neuroprotection of polyphenols with respect to resveratrol in Parkinson's Disease. *Biomedicines* <https://doi.org/10.3390/biomedicines9080918> (2021).
21. Zhou, J. et al. Beneficial effects of resveratrol-mediated inhibition of the mTOR pathway in spinal cord injury. *Neural Plast.* **2018**, 7513748 (2018).
22. Meng, T. et al. Anti-inflammatory action and mechanisms of resveratrol. *Molecules* <https://doi.org/10.3390/molecules26010229> (2021).
23. Salehi, B. et al. Resveratrol: A double-edged sword in health benefits. *Biomedicines* <https://doi.org/10.3390/biomedicines6030091> (2018).
24. Dong, Z. B. et al. Resveratrol ameliorates oxaliplatin-induced neuropathic pain via anti-inflammatory effects in rats. *Exp. Ther. Med.* **24**(3), 586 (2022).
25. Wang, B. et al. Deciphering resveratrol's role in modulating pathological pain: From molecular mechanisms to clinical relevance. *Phytother. Res.* **38**(1), 59–73 (2024).
26. Hernandez-Vazquez, L. et al. Anti-allodynic and anti-hyperalgesic activity of (+/-)-licarin A in neuropathic rats via NO-cyclic-GMP-ATP-sensitive K⁺ channel pathway. *Drug Dev. Res.* **85**(1), e22134 (2024).
27. Bennett, G. J. & Xie, Y. K. A peripheral mononeuropathy in rat that produces disorders of pain sensation like those seen in man. *Pain* **33**(1), 87–107 (1988).
28. Yin, Z. et al. ROS: Executioner of regulating cell death in spinal cord injury. *Front. Immunol.* **15**, 1330678 (2024).
29. He, L. et al. Antioxidants maintain cellular redox homeostasis by elimination of reactive oxygen species. *Cell. Physiol. Biochem.* **44**(2), 532–553 (2017).
30. Tian, Y. et al. Resveratrol as a natural regulator of autophagy for prevention and treatment of cancer. *Onco Targets Ther* **12**, 8601–8609 (2019).
31. Wu, H. et al. Resveratrol: Harnessing nature's potential for chronic pain relief. *Aging Dis.* (2025).
32. Inoue, H. & Nakata, R. Resveratrol targets in inflammation. *Endocr. Metab. Immune Disord. Drug Targets* **15**(3), 186–195 (2015).
33. Singh, K., Gupta, J. K. & Kumar, S. The pharmacological potential of resveratrol in reducing soft tissue damage in osteoarthritis patients. *Curr. Rheumatol. Rev.* **20**(1), 27–38 (2024).
34. Singh, A. P. et al. Health benefits of resveratrol: Evidence from clinical studies. *Med. Res. Rev.* **39**(5), 1851–1891 (2019).
35. Sharma, S., Chopra, K. & Kulkarni, S. K. Effect of insulin and its combination with resveratrol or curcumin in attenuation of diabetic neuropathic pain: Participation of nitric oxide and TNF-alpha. *Phytother. Res.* **21**(3), 278–83 (2007).
36. Wang, Y. et al. Resveratrol mediates mechanical allodynia through modulating inflammatory response via the TREM2-autophagy axis in SNI rat model. *J. Neuroinflammation.* **17**(1), 311 (2020).
37. Tao, L. et al. Resveratrol attenuates neuropathic pain through balancing pro-inflammatory and anti-inflammatory cytokines release in mice. *Int. Immunopharmacol.* **34**, 165–172 (2016).
38. Yao, W. et al. Recombinant protein transduction domain-Cu/Zn superoxide dismutase alleviates bone cancer pain via peroxiredoxin 4 modulation and antioxidation. *Biochem. Biophys. Res. Commun.* **486**(4), 1143–1148 (2017).
39. Recalde, M. D. et al. Resveratrol exerts anti-oxidant and anti-inflammatory actions and prevents oxaliplatin-induced mechanical and thermal allodynia. *Brain Res.* **1748**, 147079 (2020).
40. Miguel, C. A. et al. Antioxidant, anti-inflammatory and neuroprotective actions of resveratrol after experimental nervous system insults. Special focus on the molecular mechanisms involved. *Neurochem. Int.* **150**, 105188 (2021).
41. Singh, A. K. & Vinayak, M. Anti-nociceptive effect of resveratrol during inflammatory hyperalgesia via differential regulation of pro-inflammatory mediators. *Phytother. Res.* **30**(7), 1164–71 (2016).
42. Nohl, H., Gille, L. & Staniek, K. Intracellular generation of reactive oxygen species by mitochondria. *Biochem. Pharmacol.* **69**(5), 719–723 (2005).
43. Islam, M. T. Oxidative stress and mitochondrial dysfunction-linked neurodegenerative disorders. *Neurol. Res.* **39**(1), 73–82 (2017).
44. Morato, L. et al. Mitochondrial dysfunction in central nervous system white matter disorders. *Glia* **62**(11), 1878–94 (2014).
45. Zhang, H. et al. SIRT1 mediated inhibition of VEGF/VEGFR2 signaling by resveratrol and its relevance to choroidal neovascularization. *Cytokine* **76**(2), 549–552 (2015).
46. Vercellino, I. & Sazanov, L. A. The assembly, regulation and function of the mitochondrial respiratory chain. *Nat. Rev. Mol. Cell. Biol.* **23**(2), 141–161 (2022).
47. Jheng, H. F. et al. Mitochondrial fission contributes to mitochondrial dysfunction and insulin resistance in skeletal muscle. *Mol. Cell. Biol.* **32**(2), 309–19 (2012).
48. Grel, H. et al. Mitochondrial dynamics in neurodegenerative diseases: Unraveling the role of fusion and fission processes. *Int. J. Mol. Sci.* <https://doi.org/10.3390/ijms241713033> (2023).
49. Burte, F. et al. Disturbed mitochondrial dynamics and neurodegenerative disorders. *Nat. Rev. Neurol.* **11**(1), 11–24 (2015).
50. Jin, H. W. et al. Prevention of paclitaxel-evoked painful peripheral neuropathy by acetyl-L-carnitine: Effects on axonal mitochondria, sensory nerve fiber terminal arbors, and cutaneous Langerhans cells. *Exp. Neurol.* **210**(1), 229–37 (2008).
51. Zhang, K. L. et al. Targeted up-regulation of Drp1 in dorsal horn attenuates neuropathic pain hypersensitivity by increasing mitochondrial fission. *Redox Biol.* **49**, 102216 (2022).

Author contributions

Yanyan Sun designed the study and provided financial support. Liu Xie conducted behavioral tests, immunofluorescence experiments, Western blot analysis, and mitochondrial morphology assessments. Data analysis was carried out by Liu Xie, Wanting Chang, and Linna Song. The CCI model was developed by Liu Xie and Qingqing Yang. Liu Xie drafted the manuscript, which was revised by Yanyan Sun and Yiran Xu. All authors gave their approval for the final version of the manuscript.

Funding

This research was funded by the Young Scientists Fund of the National Natural Science Foundation of China (Grant No. 82203969), the Young and Middle-Aged Health Science and Technology Innovation Talent Training Program of the Henan Provincial Health Commission (Grant No. YQRC2024019), and the Clinical Medical Scientist Training Program of Henan Province (Grant No. HNCMS202433).

Declarations

Consent for publication

All authors agree to take responsibility for their contributions and have approved the submitted version of this manuscript.

Competing interests

The authors declare no competing interests.

Additional information

Supplementary Information The online version contains supplementary material available at <https://doi.org/10.1038/s41598-026-41965-7>.

Correspondence and requests for materials should be addressed to Y.S.

Reprints and permissions information is available at www.nature.com/reprints.

Publisher's note Springer Nature remains neutral with regard to jurisdictional claims in published maps and institutional affiliations.

Open Access This article is licensed under a Creative Commons Attribution-NonCommercial-NoDerivatives 4.0 International License, which permits any non-commercial use, sharing, distribution and reproduction in any medium or format, as long as you give appropriate credit to the original author(s) and the source, provide a link to the Creative Commons licence, and indicate if you modified the licensed material. You do not have permission under this licence to share adapted material derived from this article or parts of it. The images or other third party material in this article are included in the article's Creative Commons licence, unless indicated otherwise in a credit line to the material. If material is not included in the article's Creative Commons licence and your intended use is not permitted by statutory regulation or exceeds the permitted use, you will need to obtain permission directly from the copyright holder. To view a copy of this licence, visit <http://creativecommons.org/licenses/by-nc-nd/4.0/>.

© The Author(s) 2026